Atmos. Chem. Phys. Discuss., 14, 7859–7887, 2014
www.atmos-chem-phys-discuss.net/14/7859/2014/
doi:10.5194/acpd-14-7859-2014

Atmospheric Chemistry and Physics
Open Access
Discussions

Influence of biomass burning plumes on HONO chemistry in eastern China

W. Nie[1], A. J. Ding[1], Y. N. Xie[1], Z. Xu[2], H. Mao[1,4], V. Kerminen[3], L. F. Zheng[2,1], X. M. Qi[1], X. Q. Yang[1], J. N. Sun[1], E. Herrmann[1], T. Petäjä[3], M. Kulmala[3], and C. B. Fu[1]

[1]Institute for Climate and Global Change Research & School of Atmospheric Sciences, Nanjing University, Nanjing, 210093, China
[2]Environment Research Institute, Shandong University, Jinan, China
[3]Division of Atmospheric Sciences, Department of Physics, University of Helsinki, Helsinki, Finland
[4]Department of Chemistry, State University of New York College of Environmental Science and Forestry, Syracuse, New York, USA

Received: 2 March 2014 – Accepted: 8 March 2014 – Published: 21 March 2014

Correspondence to: A. J. Ding (dingaj@nju.edu.cn)

Published by Copernicus Publications on behalf of the European Geosciences Union.

Abstract

Nitrous acid (HONO) plays a key role in atmospheric chemistry via influencing the budget of hydroxyl radical (OH). In this study, a two-month measurement period of HONO and related quantities were analyzed during a biomass burning season in 2012 at a suburban site in the western Yangtze River delta, eastern China. An overall high HONO concentration with the mean value of 1.1 ppbv was observed. During biomass burning (BB) periods, both HONO concentration and HONO/NO_2 ratio were enhanced significantly compared with non-biomass burning periods. A correlation analysis showed that the HONO concentration was not associated potassium (a tracer of BB) in BB plumes, but showed a high correlation with the NO_2 concentration, suggesting a principle role of secondary production rather than direct emissions in elevated HONO concentrations. A further analysis based on comparing the surface area at similar PM levels and HONO/NO_2 ratios at similar surface area levels suggested larger specific surface areas and higher NO_2 conversion efficiencies of BB aerosols. A mixed plume of BB and anthropogenic fossil fuel (FF) emissions was observed on 10 June with even higher HONO concentrations and HONO/NO_2 ratios. The strong HONO production potential (high HONO/NO_2 to $PM_{2.5}$ ratio) was accompanied with a high sulfate concentration in this plume, suggesting a promotion of mixed aerosols to HONO formation. In summary, our study suggests an important role of BB in atmospheric oxidation capacity by affecting the HONO budget. This can be especially important in eastern China, where agricultural burning plumes are inevitably mixed with urban pollutions.

1 Introduction

Nitrous acid (HONO) is an important constituent in the troposphere due to its role in hydrogen oxides (HO_x) cycling (Platt et al., 1980; Kleffmann, 2007; Hofzumahaus et al., 2009; Elshorbany et al., 2012). The photolysis of HONO provides a daytime source of hydroxyl radical (OH), which controls the daytime oxidation capacity and consequently influences the O_3 chemistry and secondary organic aerosol (SOA) formation. This process appears especially important in the early morning when contributions from other OH sources, like ozone photolysis, are still small (Alicke et al., 2002; Kleffmann et al., 2005; Elshorbany et al., 2010).

The sources of atmospheric HONO, including direct emission from fossil fuel combustion (Kurtenbach et al., 2001) and ground surfaces (Su et al., 2011), homogeneous gas phase reactions and heterogeneous processes on the surface of atmospheric aerosols and ground (Harrison and Collins, 1998; Longfellow et al., 1999; Stutz et al., 2002; VandenBoer et al., 2013), are hitherto not well understood. Among these sources, heterogeneous processes are commonly accepted as the dominant, yet least understood, pathway to produce HONO. For example, NO_2 can be converted to HONO on ground (Harrison and Kitto, 1994) or water (Finlayson-Pitts et al., 2003) surfaces, on soot particles (Ammann et al., 1998; Kalberer et al., 1999; Kleffmann and Wiesen, 2005), or on organic substrates (Bröske et al., 2003; Ammann et al., 2005). These processes have been considered as the primary contributor to the nocturnal HONO formation, but they cannot sustain the frequently-observed elevated daytime HONO concentration levels (Kleffmann, 2007; Sorgel et al., 2011; Li et al., 2012, and the references therein). Recently, several heterogeneous and possibly photo-enhanced processes have been demonstrated that might play an important role in daytime HONO formation (George et al., 2005; Stemmler et al., 2006; Ndour et al., 2008; Nie et al., 2012). However, although these studies have drawn a clearer picture on the HONO chemistry, there are still large knowledge gabs in HONO sources. The principal process contributing to HONO formation in different chemical environments is still under debate.

Biomass burning is a major source of atmospheric aerosol particles (Janhäll et al., 2010) and trace gases (Andreae and Merlet, 2001; Burling et al., 2010), consequently influencing climate and air quality. Recent studies have connected the HONO chemistry to biomass burning via both direct HONO emissions and emissions of soot particles (Aubin and Abbatt, 2007). Although high emission ratios of HONO have been detected in the laboratory fires (Burling et al., 2010; Veres et al., 2010), the mixing ratio of HONO in aged biomass burning plumes is expected to be relatively independent of its direct emissions due to the rapid dilution and other sinks for primary HONO during the atmospheric transport. Soot particles have been demonstrated to be an effective media to convert NO_2 to HONO, yet their contribution to the atmospheric HONO budget has been thought to be negligible due to the rapid deactivation of soot surfaces under atmospheric conditions (Kleffmann et al., 1999; Aumont et al., 1999; Prince et al., 2002; Kleffmann and Wiesen, 2005; Aubin and Abbatt, 2007). However, a recent laboratory study suggested the aged soot particles can be re-actived in the present of light to enhance the HONO production (Monge et al., 2010), and play a continuous role in the HONO chemistry. These processes may significantly influence the HONO chemistry during a biomass burning period, but their exact roles are rarely demonstrated in the real atmosphere, especially when BB aerosols are mixed with anthropogenic pollutants.

In this study, a two-month measurement campaign was conducted during the intensive biomass burning (BB) period (April to June 2012) at the SORPES station (Stations for Observing Regional Processes of the Earth System) in western Yangtze River delta (YRD) of East China (Ding et al., 2013b). Several HONO-related quantities were measured, with the aim to investigate the HONO chemistry in YRD, a region undergoing rapid urbanization and industrialization. A special attention was given to the impact of BB plumes and mixed plumes of agricultural burning and fossil fuel (FF) emissions on HONO formation after a long-range transport. In the following, we will first describe the general features related to HONO during the campaign. The differences in HONO formation between the BB events and non-BB events will then be investigated. The influence of mixed plumes of intensive BB and FF emission (Ding et al., 2013a) on HONO formation will be finally discussed.

2 Experimental methodologies

2.1 Filed campaign

The field campaign was conducted from late April to June 2012 at the SORPES "flagship" central site in Xianlin (Ding et al., 2013b). It is a regional background site, located on the top of a hill (118°57′10″ E, 32°07′14″ N, 40 m a.s.l.) in the Xianlin campus of Nanjing University and about 20 km east of the suburban Nanjing city (see Fig. 1 in Ding et al., 2013b). A suite of trace gases, aerosols and meteorological quantities were measured, with more detailed descriptions found in Ding et al. (2013b). The present study is focused on HONO and related quntities, including NO_2, $PM_{2.5}$ mass, potassium ions, and particle surface-area size distribution over the size range of 6–800 nm.

2.2 Measurement techniques

The HONO concentration was measured with a Monitor for Aerosols and Gases in Air (MARGA, Metrohm Co.), which includes a wet rotating denuder (WRD) (Spindler et al., 2003; Acker et al., 2005; Su et al., 2008; Makkonen et al., 2012) connected to an ion chromatography (IC, Metrohm USA, Inc., Riverview, FL). The time resolution of this measurement is 1 h. The WRD consists of two concentric glass cylinders whose wall is coated with 10 ppm H_2O_2 solution to absorb HONO and other gases. The liquid sample streams from WRD are drawn into 25 mL syringes before injecting into the IC system. The residence time of sampling air is actually very short in the sampling tubes (about 4.5 s) and WRD (about 0.2 s), the artifact caused by the NO_2 conversion on the surface of the sampling tube and WRD solution is therefore small (Spindler et al., 2003).

Other measurement techniques are described briefly as follows. The fine particle mass concentration ($PM_{2.5}$) was continuously measured with a combined technique of light scattering photometry and beta radiation attenuation (Thermo Scientific SHARP Monitor Model 5030). Sulfate and potassium concentrations in $PM_{2.5}$ were measured with the MARGA system (Ding et al., 2013a). NO_2 was converted to NO with a heated molybdenum oxide (MoO) and measured with a chemiluminescence analyzer (TEI model 42i). The SO_2 concentration was measured with a pulsed UV fluorescence analyzer (TEI model 43i). Detailed information can be found in Ding et al. (2013b).

3 Result and discussions

3.1 Observation overview

Figure 1 shows the temporal variations of concentrations of HONO, NO_2, $PM_{2.5}$ mass and potassium observed at the Xianlin SORPES central site during the time period of April–June 2012. The average concentration of HONO was 1.1 ± 0.95 ppbv, which is comparable to the concentrations measured in a polluted rural site in the Pearl River Delta region (Su et al., 2008) and urban site in Shanghai (Wang et al., 2013), but much higher than those measured in Europe (Acker and Möller, 2007). The HONO concentration exhibited a distinct diurnal cycle with the daily peak at night and in the early morning and minimum around the noon. The average diurnal amplitude was ~ 1 ppbv (Fig. 2).

During the campaign and especially from late May to early June, several BB episodes were observed, revealed by elevated concentrations of $PM_{2.5}$ (exceeding 400 $\mu g m^{-3}$) and potassium (exceeding 20 $\mu g m^{-3}$) (Fig. 1) (Ding et al., 2013a, b). Interestingly, HONO concentrations were also significantly enhanced during the BB episodes. In order to investigate the relation between BB and HONO chemistry, we compared the HONO concentrations, $HONO/NO_2$ ratios and $HONO/NO_x$ ratios between the BB and non-BB periods. The samples with potassium concentrations higher than 2 $\mu g m^{-3}$ and the ratio of potassium to $PM_{2.5}$ larger than 0.02 were defined as BB samples, the remaining ones being categorized as non-BB samples. On average, all the three parameters of HONO concentration, $HONO/NO_2$ ratio and $HONO/NO_x$ ratios were significantly higher (about a factor of 2) during BB periods than during other times (Fig. 3), indicating a positive impact of BB on the ambient mixing ratio of HONO.

The enhanced HONO production in BB plumes would significantly impact the atmospheric oxidation capacity, and in turn influence a series of processes, like the formation of secondary aerosols (Li et al., 2010; Gonçalves et al., 2012; Elshorbany et al., 2014). In this study, the observed HONO to NO_x ratios (on average 0.045 ± 0.026), especially during BB periods (on average 0.076±0.035) (see Fig. 3c) are considerably higher than the assumed global averaged value (0.02) (Elshorbany et al., 2012, 2014), suggesting a potential more important role of HONO chemistry in the YRD, especially during the BB seasons.

3.2 Influence of BB on HONO formation

Several laboratory studies have demonstrated BB as an effective HONO source via direct emissions (Burling et al., 2010; Veres et al., 2010), so HONO might play an important role in atmospheric chemistry over BB source regions. However, HONO is a highly-reactive species that is easily consumed by chemical sinks during its atmospheric transport, especially in daytime. In this study, the main BB source area is located in the northern part of Anhui province several hundred kilometers from the SORPES station (Fig. 4). At least several hours were therefore needed before the BB emissions get to our measurement site, so the contribution of direct emissions to the observed HONO can be considered negligible. To further verify this point, we looked at the relation between HONO and potassium (Fig. 5) as well as between HONO and NO_2 (Fig. 6) during the BB periods. Results showed that HONO was poorly correlated with potassium, a tracer for direct BB emissions, but highly correlated with NO_2, suggesting the key role of chemical conversion rather than direct emissions in causing elevated HONO concentrations. Therefore, the observed high HONO concentrations during the BB periods is expected to be due to either increased precursor concentrations or increased NO_2 to HONO conversion efficiency. As shown in Fig. 1, the concentration levels of NO_2 were comparable during the BB and non-BB periods, so the higher HONO level during BB period was probably due in large part to a higher NO_2 conversion potential ($HONO/NO_2$ ratio, Fig. 3b).

Both ground and aerosols are effective surfaces for converting NO_2 to HONO. Given that there was practically no difference in the ground surface between the BB and non-BB periods during the campaign, the elevated HONO concentrations observed during BB episodes are expected to be due to aerosol-related heterogeneous processes. The enhanced aerosol particle loadings associated with the BB plumes (Fig. 1), providing large aerosol surface areas (Fig. 6), should aid the NO_2 to HONO conversion. Besides the particle mass concentration, the size distribution and morphology of aerosol particles also influence the surface area concentration. In Fig. 7, we selected the samples with the $PM_{2.5}$ mass in the concentration range 100–150 $\mu g\,m^{-3}$ during both BB and non-BB periods, and compared their surface area concentrations calculated by the size distribution. The results showed a significantly larger surface area concentration for BB aerosols compared with non-BB aerosols. This suggests that BB aerosols have a larger specific surface area than non-BB aerosol, favoring NO_2 to HONO conversion at similar levels of the PM mass concentration.

Besides the surface area concentrations, the chemical nature of aerosols is also a candidate to influence the transformation of NO_2 to HONO. We calculated the ratio between $HONO/NO_2$ and aerosol surface area in a narrow surface area concentration range, $1.5–2.2 \times 10^{-9}\,m^2\,cm^{-3}$, which overlaps measured surface area concentrations during both BB and non-BB periods. The values of this ratio were ∼ 40 % higher during the BB period than that during non-BB period (Fig. 8), indicating a higher NO_2 conversion efficiency of BB aerosols.

In summary, the elevated HONO formation observed in BB plumes was caused by the combined effects of enhanced particle loadings, higher specific aerosol surface areas, and more efficient conversion of NO_2 to HONO on particle surfaces. It is well known that high particle loadings associated with BB are caused by both primary particle emissions and secondary aerosol formation during the atmospheric transport (Andreae and Merlet, 2001; Li et al., 2003; Capes et al., 2008). Large aerosol specific surface areas are probably due to the extremely high number concentrations of accumulation mode particles during BB (Janhäll et al., 2010), and possibly the irregular shape of soot particles (Dobbins and Megaridis, 1987; Cai et al., 1993), which is one major product of BB. The higher NO_2 to HONO conversion efficiency on particle surfaces in BB plumes compared with non-BB air is a complex issue. One possible reason is the high abundance of organic (e.g. humic like) substances and soot particles (Reid et al., 2005), which are high-performance medians to convert NO_2 to HONO.

3.3 Influence of mixed plume of biomass burning and fossil fuel emissions on HONO chemistry

An intense BB episode mixed with FF emissions that significant influenced on the everyday weather was observed on 10 June 2012 (Ding et al., 2013a). Interestingly, the highest mixing ratios of HONO, exceeding 5 ppbv, occurred during this episode (Fig. 1). The solar radiation intensity was significantly decreased in the daytime of this episode due to the extremely high particle loading (see Fig. 3 in Ding et al., 2013a), and HONO concentrations during the daytime were at a similar level as those during the nighttime. Although a high particle loading should be a contributor to the high HONO levels, it was not likely the most predominant factor because the PM concentrations during this event were comparable to the peak concentrations during the other BB episodes (Fig. 1).

Figure 9 shows the scatter plot between HONO and NO_2 concentrations during the BB periods. The dataset was separated into two groups: the beginning stage of 10 June (red squares, first 4–5 h) combined with other BB episodes (blue squares) and later stage of 10 June (green circle dots). Both groups reveal a strong relation between HONO and NO_2 with the correlation coefficient higher than 0.8. The slope of the regression of the latter stage of 10 June is almost a factor of 2 higher (0.15) than that for the other group (0.08, mostly the data points of other BB episodes), indicating a higher NO_2 to HONO conversion potential of the aerosols in the later stage of 10 June case compared with other BB episodes. To further verify this point and exclude the influence of particle loading, samples with $PM_{2.5}$ concentration in range of 200–300 $\mu g\,m^{-3}$ (the overlapping parts) were selected from both these groups. Although the selected samples had similar PM concentration levels, the HONO/NO_2 ratios and rations between

$HONO/NO_2$ and $PM_{2.5}$ were much higher during 10 June than those during the other BB episodes, indicating a higher potential for the aerosols on 10 June case to convert NO_2 to HONO. It should be noted that the dataset of surface area during the 10 June case was not available because the extremely high particle loading influenced the sample inlet of the DMPS. The exact contributors to the enhancement of NO_2 conversion potentials, which is either higher specific aerosol surface areas or stronger conversion efficient, are therefore not clear.

Our previous study demonstrated that the episode on 10 June was caused not only by the BB but a mixture of intense BB and anthropogenic FF emissions (Ding et al., 2013a). As shown in Fig. 11, the SO_2 concentration was low at the beginning stage of this episode and then gradually increased, suggesting the mixing of anthropogenic pollutions rich in SO_2 with the BB particles several hours after the invasion of the BB plume. This is why the chemical features ($HONO/NO_2$) in the plume of the beginning stage of the 10 June case was similar to that in other BB episodes, yet very different from the later stage of the 10 June case (Fig. 9).

The mix of BB plumes and FF emissions will promote the formation of secondary aerosols (e.g. sulfate and secondary organic aerosols, SOA) on BB particles, and thus modify their morphology and surface chemical nature (Li et al., 2003; Capes et al., 2008). As shown in Fig. 10d, the abundance of sulfate in $PM_{2.5}$ was significantly enhanced on 10 June case compared with other BB episodes. This coincided with the high NO_2 to HONO conversion efficiency (Fig. 10c), indicating a promotion of secondary aerosol formation on BB particles in the mixed plumes to produce HONO. To further verify this point, we plotted the nighttime HONO against the sulfate concentration on 10 June (Fig. 12), noting that the daytime HONO chemistry is out of the scope of this work. The result show a very good correlation between the two species ($R = 0.79$), further suggesting the promotion of secondary aerosol formation on BB particles to HONO formation.

As discussed above, the specific surface area and chemical nature of aerosol particles are the key factors in determining their potential to convert NO_2 to HONO. Therefore, changes in the morphology and size distribution caused by secondary aerosol formation may have enhanced the specific surface area and led to increased HONO production in the mixed plumes. Another factor that might enhance HONO production might be the formation of some specific secondary material on BB particles. It should be noted that sulfate is only a tracer for new-formed secondary species here, with no direct evidence on sulfate being a productive media for converting NO_2 to HONO. Instead, the secondary organic aerosols are more likely the contributor (Bröske et al., 2003). Finally, the enhanced RH aerosol water content (Fig. 11) caused by the production of hydrophilic species, e.g. sulfate, may also play a role in accelerating the NO_2 conversion (Stutz et al., 2004).

4 Conclusions

In this study, we analyzed a two-month measurement period of atmospheric HONO during the BB season of 2012 (May and June) at the SORPES central site in western YRD of eastern China, and demonstrated an important role of BB in the HONO chemistry in the ambient atmosphere. HONO formation was detected to be significantly elevated during the BB periods due to combined effect of enhanced particle loadings, larger specific surface areas of particles and higher NO_2 conversion efficiency on BB aerosols. An episode of the mixed plumes of intense BB and anthropogenic FF emissions was observed on 10 June, during which the HONO production potentials from the conversion of NO_2 was further promoted by the formation of secondary particulate matter on BB particles. Given that BB plumes are easily mixed with other anthropogenic pollutants in eastern China, their influences on the atmospheric oxidation capacity is expected to be important via affecting the HONO budget and thus the radical pool. Furthermore, considering the potential re-activation of BB particles (e.g. soot) during their atmospheric transport, the HONO chemistry associated with BB plumes may affect atmospheric chemistry long distances downwind BB areas, even in the marine boundary layer. Therefore, more studies are encouraged on BB related chemistry in eastern China, which is a unique “laboratory” with frequent mixed plumes of BB and anthropogenic pollutions.

Acknowledgements. This work was funded by National Natural Science Foundation of China (D0512/0207131138 and D0510/41275129), the MOST 973 Program (2010CB428500), and the Jiangsu Provincial 2011 Program (Collaborative Innovation Center of Climate Change). The SORPES-NJU stations were supported by the 985 Program and the Fundamental Research Funds for Central Universities from Ministry of Education, China. We thank T. Wang and L. Xue at The Hong Kong Polytechnic University for their suggestion on the data analysis. We are grateful of J. Kleffmann at Bergische Universität Wuppertal for his useful discussions on the data quality. We thank Metrohm Co. China for providing the MARGA analyzer and Z. Yan and J. Gao for their technical support for the instrument.

References

Acker, K. and Möller, D.: Atmospheric variation of nitrous acid at different sites in Europe, Environ. Chem., 4, 242–255, doi:10.1071/EN07023, 2007.

Acker, K., Möller, D., Auel, R., Wieprecht, W., and Kalaß, D.: Concentrations of nitrous acid, nitric acid, nitrite and nitrate in the gas and aerosol phase at a site in the emission zone during ESCOMPTE 2001 experiment, Atmos. Res., 74, 507–524, doi:10.1016/j.atmosres.2004.04.009, 2005.

Alicke, B., Platt, U., and Stutz, J.: Impact of nitrous acid photolysis on the total hydroxyl radical budget during the Limitation of Oxidant Production/Pianura Padana Produzione di Ozono study in Milan, J. Geophys. Res.-Atmos., 107, 8196, doi:10.1029/2000JD000075, 2002.

Ammann, M., Kalberer, M., Jost, D. T., Tobler, L., Rossler, E., Piguet, D., Gaggeler, H. W., and Baltensperger, U.: Heterogeneous production of nitrous acid on soot in polluted air masses, Nature, 395, 157–160, 1998.

Ammann, M., Rössler, E., Strekowski, R., and George, C.: Nitrogen dioxide multiphase chemistry: uptake kinetics on aqueous solutions containing phenolic compounds, Phys. Chem. Chem. Phys., 7, 2513–2518, 2005.

Andreae, M. O. and Merlet, P.: Emission of trace gases and aerosols from biomass burning, Global Biogeochem. Cy., 15, 955–966, doi:10.1029/2000gb001382, 2001.

Aubin, D. G. and Abbatt, J. P. D.: Interaction of NO_2 with hydrocarbon soot? Focus on HONO yield, surface modification, and mechanism, J. Phys. Chem. A, 111, 6263–6273, doi:10.1021/jp068884h, 2007.

Aumont, B., Madronich, S., Ammann, M., Kalberer, M., Baltensperger, U., Hauglustaine, D., and Brocheton, F.: On the NO_2 + soot reaction in the atmosphere, J. Geophys. Res.-Atmos., 104, 1729–1736, doi:10.1029/1998jd100023, 1999.

Bröske, R., Kleffmann, J., and Wiesen, P.: Heterogeneous conversion of NO_2 on secondary organic aerosol surfaces: A possible source of nitrous acid (HONO) in the atmosphere?, Atmos. Chem. Phys., 3, 469–474, doi:10.5194/acp-3-469-2003, 2003.

Burling, I. R., Yokelson, R. J., Griffith, D. W. T., Johnson, T. J., Veres, P., Roberts, J. M., Warneke, C., Urbanski, S. P., Reardon, J., Weise, D. R., Hao, W. M., and de Gouw, J.: Laboratory measurements of trace gas emissions from biomass burning of fuel types from the southeastern and southwestern United States, Atmos. Chem. Phys., 10, 11115–11130, doi:10.5194/acp-10-11115-2010, 2010.

Cai, J., Lu, N., and Sorensen, C. M.: Comparison of size and morphology of soot aggregates as determined by light scattering and electron microscope analysis, Langmuir, 9, 2861–2867, doi:10.1021/la00035a023, 1993.

Capes, G., Johnson, B., McFiggans, G., Williams, P. I., Haywood, J., and Coe, H.: Aging of biomass burning aerosols over West Africa: aircraft measurements of chemical composition, microphysical properties, and emission ratios, J. Geophys. Res.-Atmos., 113, D00C15, doi:10.1029/2008JD009845, 2008.

Ding, A. J., Fu, C. B., Yang, X. Q., Sun, J. N., Petäjä, T., Kerminen, V.-M., Wang, T., Xie, Y., Herrmann, E., Zheng, L. F., Nie, W., Liu, Q., Wei, X. L., and Kulmala, M.: Intense atmospheric pollution modifies weather: a case of mixed biomass burning with fossil fuel combustion pollution in eastern China, Atmos. Chem. Phys., 13, 10545–10554, doi:10.5194/acp-13-10545-2013, 2013a.

Ding, A. J., Fu, C. B., Yang, X. Q., Sun, J. N., Zheng, L. F., Xie, Y. N., Herrmann, E., Nie, W., Petäjä, T., Kerminen, V.-M., and Kulmala, M.: Ozone and fine particle in the western Yangtze River Delta: an overview of 1 yr data at the SORPES station, Atmos. Chem. Phys., 13, 5813–5830, doi:10.5194/acp-13-5813-2013, 2013b.

Dobbins, R. and Megaridis, C.: Morphology of flame-generated soot as determined by thermophoretic sampling, Langmuir, 3, 254–259, 1987.

Elshorbany, Y., Barnes, I., Becker, K. H., Kleffmann, J., and Wiesen, P.: Sources and cycling of tropospheric hydroxyl radicals – an overview, Int. J. Res. Phys. Chem. Chem. Phys., 224, 967–987, 2010.

Elshorbany, Y. F., Steil, B., Brühl, C., and Lelieveld, J.: Impact of HONO on global atmospheric chemistry calculated with an empirical parameterization in the EMAC model, Atmos. Chem. Phys., 12, 9977–10000, doi:10.5194/acp-12-9977-2012, 2012.

Elshorbany, Y. F., Crutzen, P. J., Steil, B., Pozzer, A., Tost, H., and Lelieveld, J.: Global and regional impacts of HONO on the chemical composition of clouds and aerosols, Atmos. Chem. Phys., 14, 1167–1184, doi:10.5194/acp-14-1167-2014, 2014.

George, C., Strekowski, R. S., Kleffmann, J., Stemmler, K., and Ammann, M.: Photoenhanced uptake of gaseous NO_2 on solid organic compounds: a photochemical source of HONO?, Faraday Discuss., 130, 195–210, doi:10.1039/b417888m, 2005.

Gonçalves, M., Dabdub, D., Chang, W. L., Jorba, O., and Baldasano, J. M.: Impact of HONO sources on the performance of mesoscale air quality models, Atmos. Environ., 54, 168–176, doi:10.1016/j.atmosenv.2012.02.079, 2012.

Harrison, R. and Collins, G.: Measurements of reaction coefficients of NO_2 and HONO on aerosol particles, J. Atmos. Chem., 30, 397–406, doi:10.1023/a:1006094304069, 1998.

Harrison, R. M. and Kitto, A.-M. N.: Evidence for a surface source of atmospheric nitrous acid, Atmos. Environ., 28, 1089–1094, doi:10.1016/1352-2310(94)90286-0, 1994.

Hofzumahaus, A., Rohrer, F., Lu, K., Bohn, B., Brauers, T., Chang, C.-C., Fuchs, H., Holland, F., Kita, K., Kondo, Y., Li, X., Lou, S., Shao, M., Zeng, L., Wahner, A., and Zhang, Y.: Amplified Trace Gas Removal in the Troposphere, Science, 324, 1702–1704, doi:10.1126/science.1164566, 2009.

Janhäll, S., Andreae, M. O., and Pöschl, U.: Biomass burning aerosol emissions from vegetation fires: particle number and mass emission factors and size distributions, Atmos. Chem. Phys., 10, 1427–1439, doi:10.5194/acp-10-1427-2010, 2010.

Kalberer, M., Ammann, M., Arens, F., Gäggeler, H. W., and Baltensperger, U.: Heterogeneous formation of nitrous acid (HONO) on soot aerosol particles, J. Geophys. Res.-Atmos., 104, 13825–13832, doi:10.1029/1999jd900141, 1999.

Kleffmann, J.: Daytime sources of nitrous acid (HONO) in the atmospheric boundary layer, Chem. Phys. Chem., 8, 1137–1144, 2007.

Kleffmann, J. and Wiesen, P.: Heterogeneous conversion of NO_2 and NO on HNO_3 treated soot surfaces: atmospheric implications, Atmos. Chem. Phys., 5, 77–83, doi:10.5194/acp-5-77-2005, 2005.

Kleffmann, J., Becker, H. K., Lackhoff, M., and Wiesen, P.: Heterogeneous conversion of NO_2 on carbonaceous surfaces, Phys. Chem. Chem. Phys., 1, 5443–5450, doi:10.1039/a905545b, 1999.

Kleffmann, J., Gavriloaiei, T., Hofzumahaus, A., Holland, F., Koppmann, R., Rupp, L., Schlosser, E., Siese, M., and Wahner, A.: Daytime formation of nitrous acid: a major source of OH radicals in a forest, Geophys. Res. Lett., 32, L05818, doi:10.1029/2005GL022524, 2005.

Kurtenbach, R., Becker, K. H., Gomes, J. A. G., Kleffmann, J., Lörzer, J. C., Spittler, M., Wiesen, P., Ackermann, R., Geyer, A., and Platt, U.: Investigations of emissions and heterogeneous formation of HONO in a road traffic tunnel, Atmos. Environ., 35, 3385–3394, doi:10.1016/S1352-2310(01)00138-8, 2001.

Li, G., Lei, W., Zavala, M., Volkamer, R., Dusanter, S., Stevens, P., and Molina, L. T.: Impacts of HONO sources on the photochemistry in Mexico City during the MCMA-2006/MILAGO Campaign, Atmos. Chem. Phys., 10, 6551–6567, doi:10.5194/acp-10-6551-2010, 2010.

Li, J., Pósfai, M., Hobbs, P. V., and Buseck, P. R.: Individual aerosol particles from biomass burning in southern Africa: 2, Compositions and aging of inorganic particles, J. Geophys. Res.-Atmos., 108, 8484, doi:10.1029/2002JD002310, 2003.

Li, X., Brauers, T., Häseler, R., Bohn, B., Fuchs, H., Hofzumahaus, A., Holland, F., Lou, S., Lu, K. D., Rohrer, F., Hu, M., Zeng, L. M., Zhang, Y. H., Garland, R. M., Su, H., Nowak, A., Wiedensohler, A., Takegawa, N., Shao, M., and Wahner, A.: Exploring the atmospheric chemistry of nitrous acid (HONO) at a rural site in Southern China, Atmos. Chem. Phys., 12, 1497–1513, doi:10.5194/acp-12-1497-2012, 2012.

Longfellow, C. A., Ravishankara, A. R., and Hanson, D. R.: Reactive uptake on hydrocarbon soot: focus on NO_2, J. Geophys. Res.-Atmos., 104, 13833–13840, doi:10.1029/1999jd900145, 1999.

Makkonen, U., Virkkula, A., Mäntykenttä, J., Hakola, H., Keronen, P., Vakkari, V., and Aalto, P. P.: Semi-continuous gas and inorganic aerosol measurements at a Finnish urban site: comparisons with filters, nitrogen in aerosol and gas phases, and aerosol acidity, Atmos. Chem. Phys., 12, 5617–5631, doi:10.5194/acp-12-5617-2012, 2012.

Monge, M. E., D'Anna, B., Mazri, L., Giroir-Fendler, A., Ammann, M., Donaldson, D. J., and George, C.: Light changes the atmospheric reactivity of soot, P. Natl. Acad. Sci. USA, 107, 6605–6609, doi:10.1073/pnas.0908341107, 2010.

Ndour, M., D'Anna, B., George, C., Ka, O., Balkanski, Y., Kleffmann, J., Stemmler, K., and Ammann, M.: Photoenhanced uptake of NO_2 on mineral dust: laboratory experiments and model simulations, Geophys. Res. Lett., 35, L05812, doi:10.1029/2007gl032006, 2008.

Nie, W., Wang, T., Xue, L. K., Ding, A. J., Wang, X. F., Gao, X. M., Xu, Z., Yu, Y. C., Yuan, C., Zhou, Z. S., Gao, R., Liu, X. H., Wang, Y., Fan, S. J., Poon, S., Zhang, Q. Z., and Wang, W. X.: Asian dust storm observed at a rural mountain site in southern China: chemical evolution and heterogeneous photochemistry, Atmos. Chem. Phys., 12, 11985–11995, doi:10.5194/acp-12-11985-2012, 2012.

Platt, U., Perner, D., Harris, G., Winer, A., and Pitts, J.: Observations of nitrous acid in an urban atmosphere by differential optical absorption, Nature, 285, 312–314, doi:10.1038/285312a0, 1980.

Prince, A. P., Wade, J. L., Grassian, V. H., Kleiber, P. D., and Young, M. A.: Heterogeneous reactions of soot aerosols with nitrogen dioxide and nitric acid: atmospheric chamber and Knudsen cell studies, Atmos. Environ., 36, 5729–5740, doi:10.1016/S1352-2310(02)00626-X, 2002.

Reid, J. S., Koppmann, R., Eck, T. F., and Eleuterio, D. P.: A review of biomass burning emissions part II: intensive physical properties of biomass burning particles, Atmos. Chem. Phys., 5, 799–825, doi:10.5194/acp-5-799-2005, 2005.

Sörgel, M., Regelin, E., Bozem, H., Diesch, J.-M., Drewnick, F., Fischer, H., Harder, H., Held, A., Hosaynali-Beygi, Z., Martinez, M., and Zetzsch, C.: Quantification of the unknown HONO daytime source and its relation to NO_2, Atmos. Chem. Phys., 11, 10433–10447, doi:10.5194/acp-11-10433-2011, 2011.

Spindler, G., Hesper, J., Brüggemann, E., Dubois, R., Müller, T., and Herrmann, H.: Wet annular denuder measurements of nitrous acid: laboratory study of the artefact reaction of NO_2 with S(IV) in aqueous solution and comparison with field measurements, Atmos. Environ., 37, 2643–2662, doi:10.1016/S1352-2310(03)00209-7, 2003.

Stemmler, K., Ammann, M., Donders, C., Kleffmann, J., and George, C.: Photosensitized reduction of nitrogen dioxide on humic acid as a source of nitrous acid, Nature, 440, 195–198, 2006.

Stutz, J., Alicke, B., and Neftel, A.: Nitrous acid formation in the urban atmosphere: gradient measurements of NO_2 and HONO over grass in Milan, Italy, J. Geophys. Res.-Atmos, 107, 8192, doi:10.1029/2001JD000390, 2002.

Stutz, J., Alicke, B., Ackermann, R., Geyer, A., Wang, S., White, A. B., Williams, E. J., Spicer, C. W., and Fast, J. D.: Relative humidity dependence of HONO chemistry in urban areas, J. Geophys. Res.-Atmos., 109, D03307, doi:10.1029/2003JD004135, 2004.

Su, H., Cheng, Y. F., Shao, M., Gao, D. F., Yu, Z. Y., Zeng, L. M., Slanina, J., Zhang, Y. H., and Wiedensohler, A.: Nitrous acid (HONO) and its daytime sources at a rural site during the 2004 PRIDE-PRD experiment in China, J. Geophys. Res.-Atmos., 113, D14312, doi:10.1029/2007jd009060, 2008.

Su, H., Cheng, Y., Oswald, R., Behrendt, T., Trebs, I., Meixner, F. X., Andreae, M. O., Cheng, P., Zhang, Y., and Pöschl, U.: Soil Nitrite as a Source of Atmospheric HONO and OH Radicals, Science, 333, 1616–1618, doi:10.1126/science.1207687, 2011.

VandenBoer, T. C., Brown, S. S., Murphy, J. G., Keene, W. C., Young, C. J., Pszenny, A. A. P., Kim, S., Warneke, C., de Gouw, J. A., Maben, J. R., Wagner, N. L., Riedel, T. P., Thornton, J. A., Wolfe, D. E., Dubé, W. P., Öztürk, F., Brock, C. A., Grossberg, N., Lefer, B., Lerner, B., Middlebrook, A. M., and Roberts, J. M.: Understanding the role of the ground surface in HONO vertical structure: high resolution vertical profiles during NACHTT-11, J. Geophys. Res.-Atmos., 118, 10155–10171, doi:10.1002/jgrd.50721, 2013.

Veres, P., Roberts, J. M., Burling, I. R., Warneke, C., de Gouw, J., and Yokelson, R. J.: Measurements of gas-phase inorganic and organic acids from biomass fires by negative-ion proton-transfer chemical-ionization mass spectrometry, J. Geophys. Res.-Atmos., 115, D23302, doi:10.1029/2010jd014033, 2010.

Wang, S., Zhou, R., Zhao, H., Wang, Z., Chen, L., and Zhou, B.: Long-term observation of atmospheric nitrous acid (HONO) and its implication to local NO_2 levels in Shanghai, China, Atmos. Environ., 77, 718–724, doi:10.1016/j.atmosenv.2013.05.071, 2013.

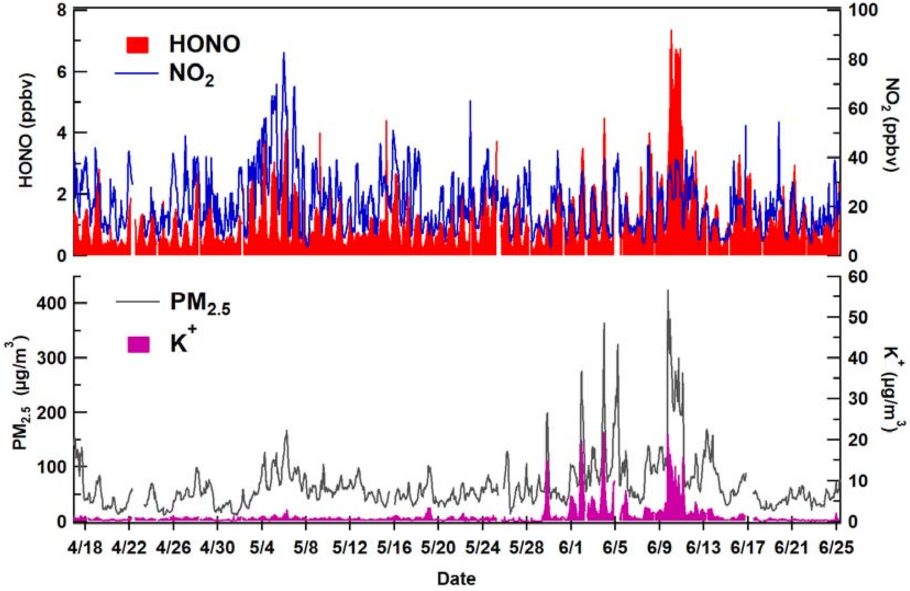

Fig. 1. Temporal variation of the concentrations of HONO, NO$_2$ PM$_{2.5}$ mass and potassium, at the SORPES central site during April to June 2009.

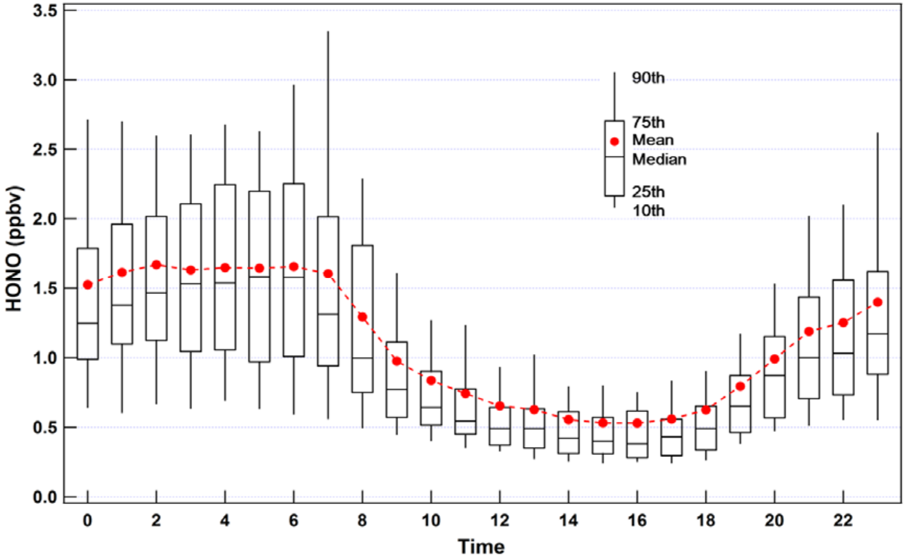

Fig. 2. Whisker plot of diurnal variation of HONO at the SORPES central site during April to June 2012.

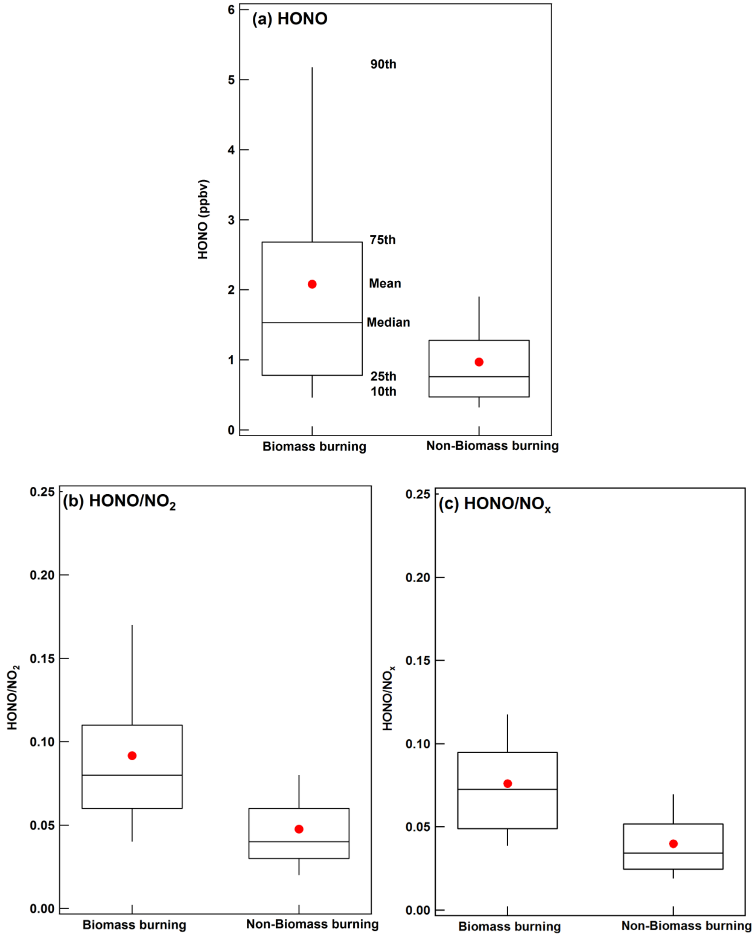

Fig. 3. Comparisons of **(a)** HONO concentrations, **(b)** HONO to NO_2 ratio and **(c)** HONO to NO_x ratio between biomass burning period and non-biomass burning period.

ACPD
14, 7859–7887, 2014

Title Page
Abstract | Introduction
Conclusions | References
Tables | Figures
◀▮ | ▶▮
◀ | ▶
Back | Close
Full Screen / Esc

Printer-friendly Version
Interactive Discussion

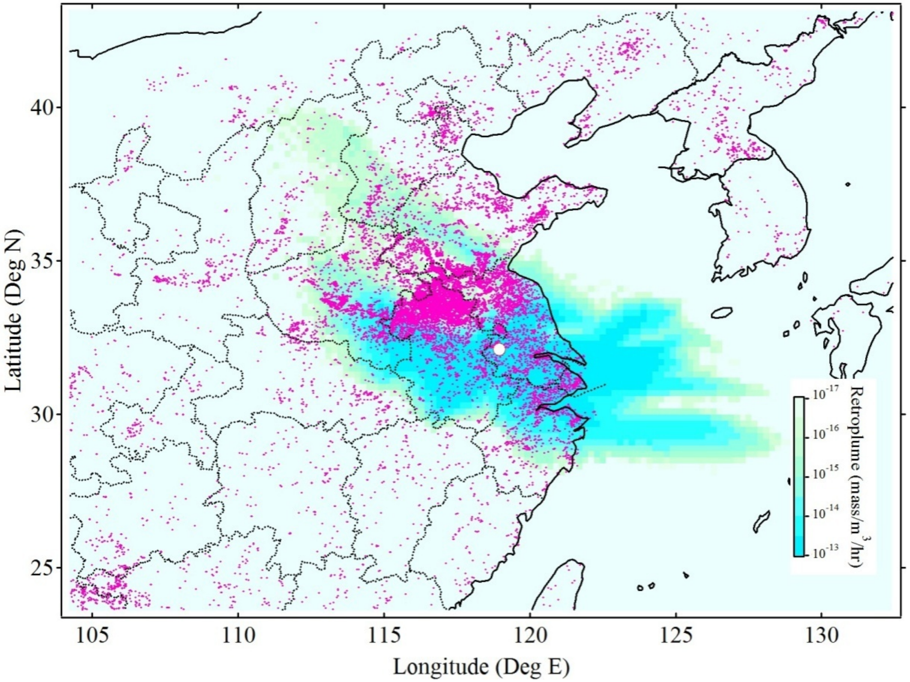

Fig. 4. Map of 24 h Lagrangian backward retroplume (100 m footprint layer) for biomass burning air masses (defined as $K^+ > 2\,\mu g\,m^{-3}$ and $K^+/PM > 2\,\%$) and active fire (pink dots) during 15 April–25 June 2012 (data obtained from FIRMS MODIS Fire Archive).

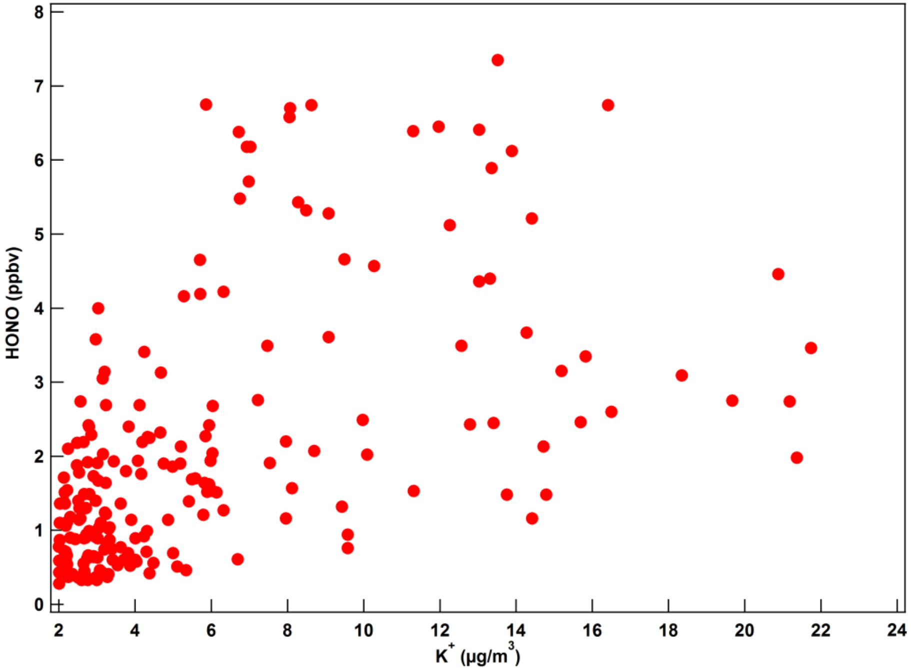

Fig. 5. Scatter plot between the HONO and potassium concentration during biomass burning periods.

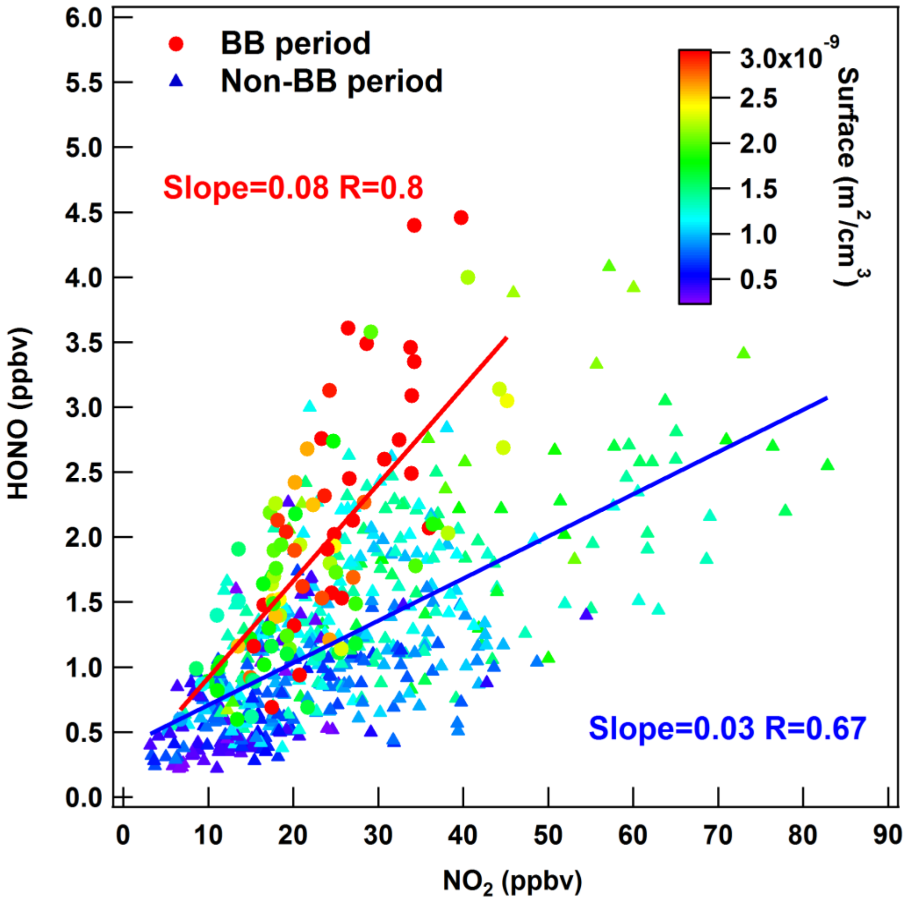

Fig. 6. Scatter plot between the HONO and NO_2 concentration during the BB periods (without the case on 10 June, red circles) and non-BB periods (blue triangles) with the particle surface area concentrations (6–800 nm) as the color scale.

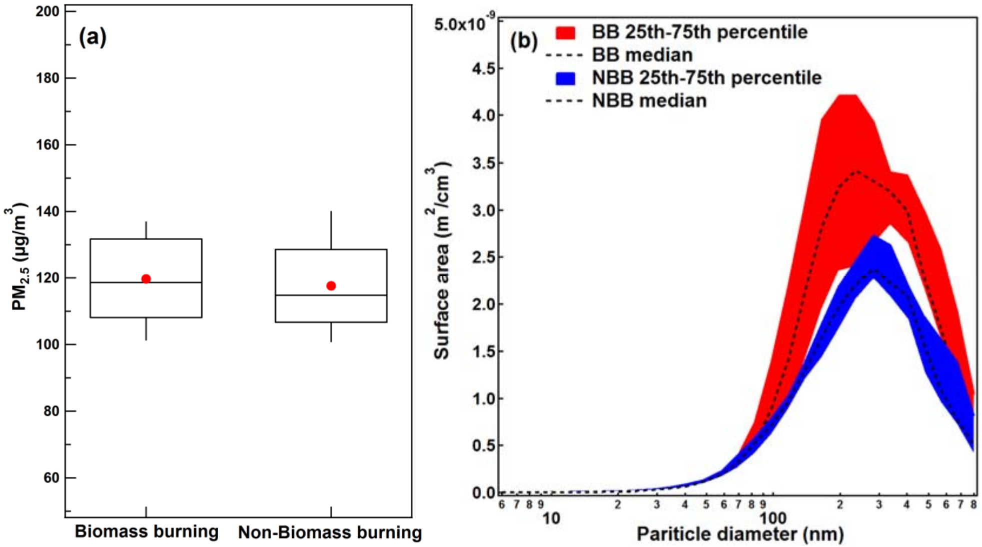

Fig. 7. (a) Whisker plot of $PM_{2.5}$ in the selected mass concentration range (100–150 μg m^{-3}) during BB and non-BB period, and **(b)** particle surface area size distributions for the same subsets of data.

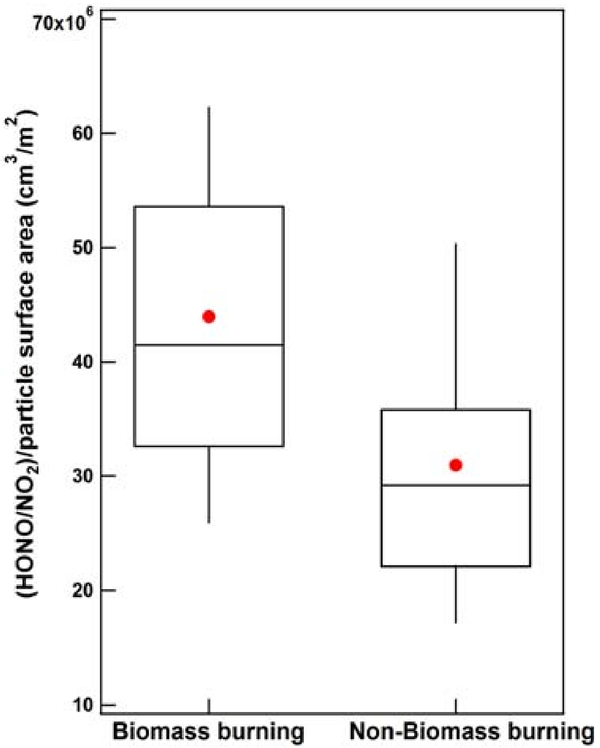

Fig. 8. Whisker plot of the ratios between HONO/NO_2 and particle surface area concentration in the selected particle surface area range (1.5–$2.2 \times 10^{-9}\,m^2\,cm^{-3}$) during the BB and non-BB periods.

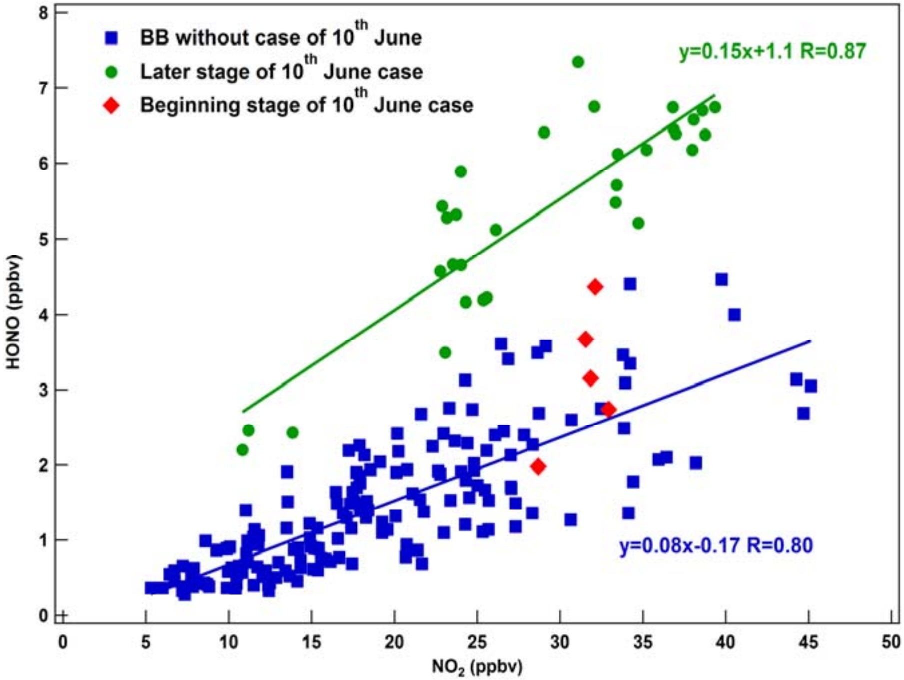

Fig. 9. Scatter plot between HONO and NO_2 concentration during the BB periods (without the case of 10 June, blue solid squares), the beginning (red solid diamonds) and latter (green dots) state of the 10 June episode.

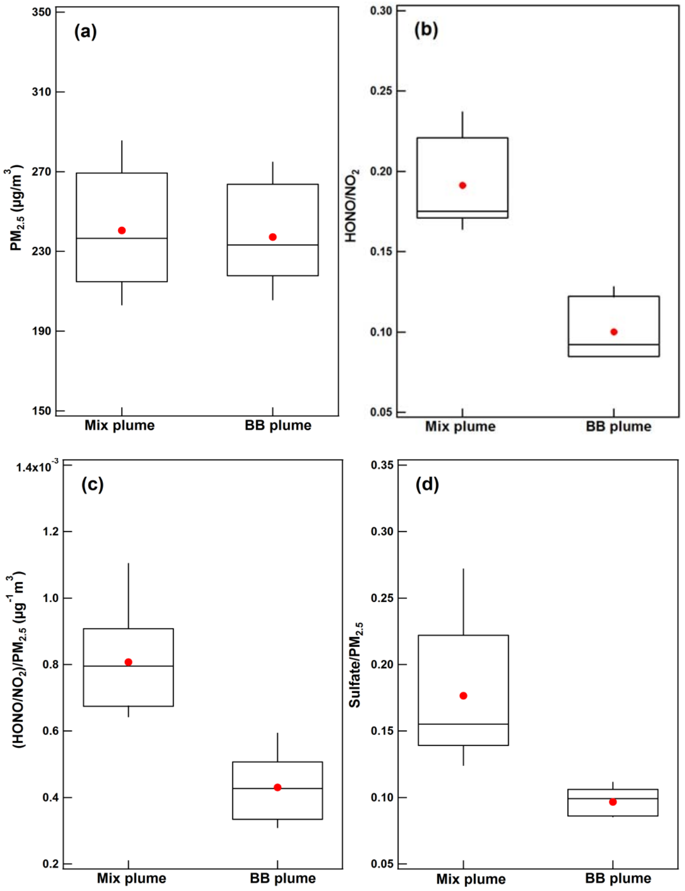

Fig. 10. Whisker plots of **(a)** $PM_{2.5}$ mass, **(b)** ratios of HONO to NO_2, **(c)** ratios of HONO/NO_2 to $PM_{2.5}$ mass, **(d)** ratios of sulfate to $PM_{2.5}$, in the selected $PM_{2.5}$ mass concentration range (150–300 $\mu g\,m^{-3}$) in the mixed plume and BB plume.

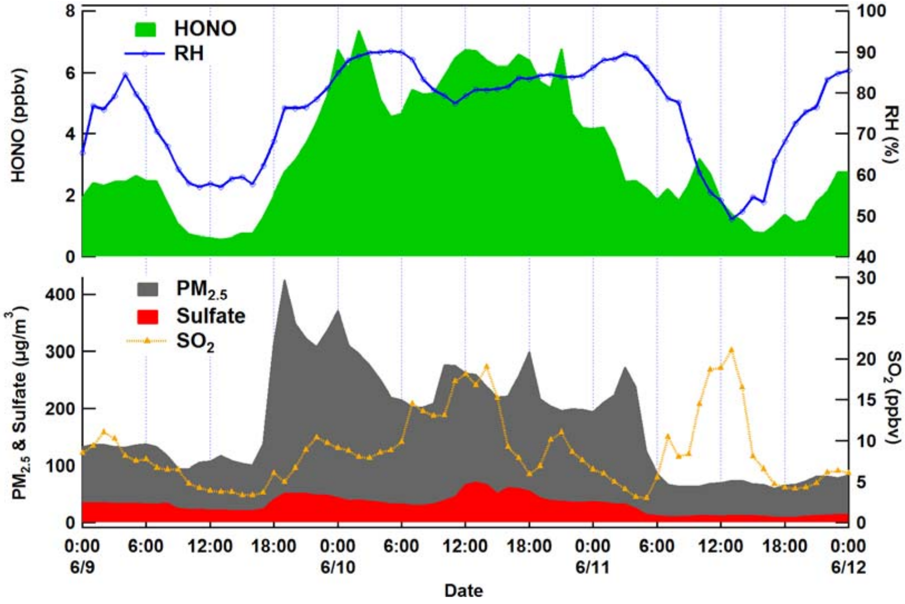

Fig. 11. Temporal variations of HONO, RH, $PM_{2.5}$, sulfate in $PM_{2.5}$ and SO_2 during 9–11 June 2012 at the SORPES central site.

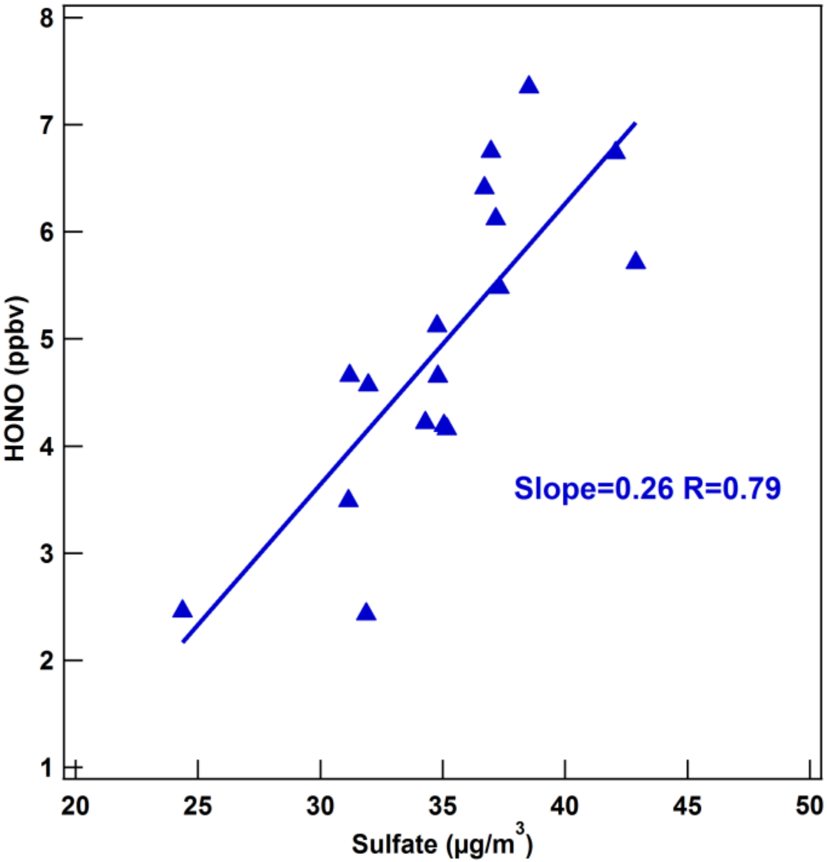

Fig. 12. Scatter plot between HONO and sulfate concentration in $PM_{2.5}$ during the nighttime on 10 June.